Finite Element Modeling of mAEWing1 in MSC PATRAN/NASTRAN

Wei Zhao[*], Rakesh K. Kapania[†],

Neeharika Muthirevula[‡] and Rikin Gupta[§]

Virginia Polytechnic Institute and State University, Blacksburg, VA, 24061

March, 2015	V1.0	April, 2015	V1.1

Note: This report draft is subject to update based on the mAEWing1 test data

[*] Graduate Research Assistant, Department of aerospace and ocean engineering, weizhao@vt.edu
[†] Mitchell Professor, Department of aerospace and ocean engineering, rkapania@vt.edu
[‡] Graduate Research Assistant, Department of aerospace and ocean engineering
[§] Graduate Research Assistant, Department of aerospace and ocean engineering,

Contents

Figures

Tables

A. Introduction

A refined finite element model will lead to a large order matrix in both stiffness and mass matrices, which will result in a very expensive computational analysis in preliminary aircraft design. Generally, a simplified beam-rod finite element model is used for the aircraft design phase as shown Figure 1, and then a refined finite element model which includes the beam elements, the shell elements, possibly the solid elements and connectors for detailed finite element analysis for stress distribution and any other interested structural responses.

Figure 1 Equivalent beam-rod finite element model used to represent the full airplane model

A simplified beam-rod model for mAEWing1 is considered for this project. This is due to the fact the main structural load carry member composes of solid composite spar in the mAEWing1 design. Also, the beam-rod finite element model provides a small order of stiffness and mass matrices in the control law design and MDAO work, which result in a cheaper and more efficient computational analysis.

B. Review of mAEWing1 CAD model

A CAD model developed in SolidWorks from UMN was provided to VT for mAEWing1 finite element modeling. The plot and summary of geometry and mass properties of mAEWing1 provided by UMN as shown below:

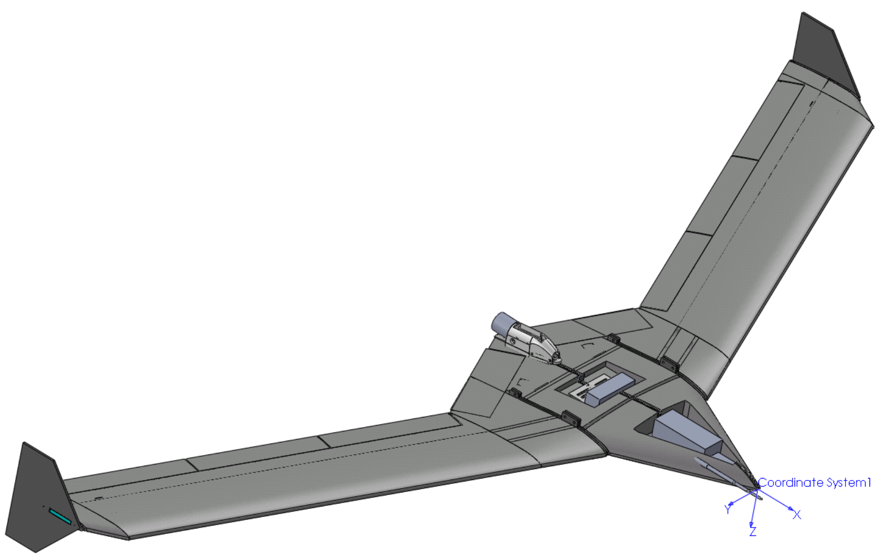

Figure 2 CAD model of mAEWing1

1) mAEWing1 Aircraft Data v0.3**

There is a summary of relevant aircraft data for mAEWing1. This data is from the mAEWing1 CAD and the BFF aircraft; subsequent versions of aircraft data of

** Provided by Chris Regan from UMN

mAEWing1 will be updated based on data that is measured during the testing mAEWing1.

a) Geometry

mAEWing1 CAD model provides dimensions for the aircraft and Spar Build and Test gives material properties. A summary of reference lengths to be used with mAEWing1 is below.

Table 1 Geometry of wing

Wing area, *S*	11.679 ft^2 (1.085 m^2)
Reference chord, *c*	1.312 ft (0.4 m)
Reference span, *b*	10 ft (3.048 m)

b) Mass Properties

Table 2 lists the summary of the aircraft mass properties to be used with mAEWing1. This information is from testing the BFF aircraft. More information regarding the mass and center of gravity can be found here: http://hdl.handle.net/11299/164145

Please note that while there is a lot of confidence in the pitch inertia, we have much less confidence in the roll and yaw inertia. Additional information regarding the aircraft inertias can be found here: http://hdl.handle.net/11299/167676

Table 2 Predicted mass properties for mAEWing1

Weight	11.99 lbs (53.334 N)
Mass	0.3727 slugs (5.4386 kg)
Longitudinal Center of Gravity	23.2585 inches (59.077 cm) aft from nose
Iyy	1245.83 lb-in^2 (0.3646 kg-m^2)
Ixx	8543.50 lb-in^2 (2.5002 kg-m^2)
Izz	8118.42 lb-in^2 (2.3758 kg-m^2)
Ixz (estimated)	0

Point masses and locations are given in mAEWing1 CAD and Spar Build and Test.

All actuators are anticipated to be the Futaba S9254 with a bandwidth of 10.5 Hz.

We are anticipating the motor for mAEWing1 to switch to the Eflite 46 or Eflite 52 from the Hacker A40-12S that is in the CAD.

C. Finite element modeling

1) Modeling of Wing

Figure 3 shows the semi-wing CAD model of mAEWing1. Based on the spar built and test report [3], 3 plies of carbon fiber fabric (Fiberglass 3K PW) was used as reinforcement. Fiberglass 2000/2060 Epoxy was used as the matrix.

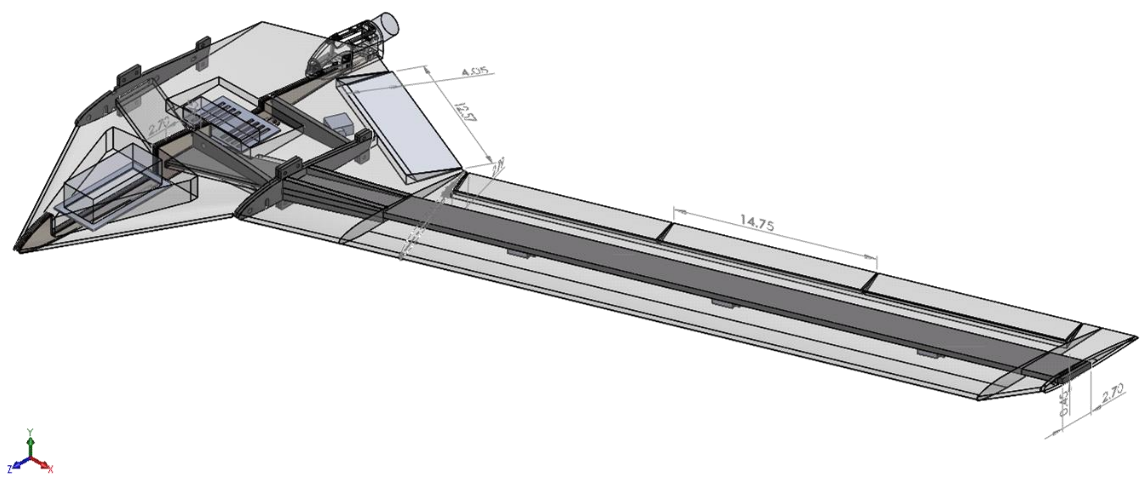

Figure 3 Semi CAD model of mAEWing1

The wing for the mAEWing1 mainly consists of solid spar and foam cover, the solid spar is modeled as a composite beam element in which the equivalent bending stiffness and torsional stiffness are considered. The Timoshenko beam theory in which the equivalent beam stiffness, out of plane bending stiffness, EI, and torsional stiffness, GJ, is used for the spar modeling. EI and GJ of the solid composite spar are obtained from the spar built and test report provided by UMN[2] as tabulated in Table 3.

Table 3 Spar Estimated Properties[††]

	EI (N-m^2)	E (GPa)	GJ (N-m^2)	G (GPa)
Predicted	97.43	45.92	59.13	8.63

From the Table 3, we can calculate the equivalent values for the out of plane area moments of inertia and torsional constants,

$$I = \frac{EI}{E} = \frac{97.43\ N\,m^2}{45.92 \times 10^9 Pa} = 2.12173 \times 10^{-9}\ m^4$$

$$J = \frac{GJ}{G} = \frac{59.13\ N\,m^2}{8.63 \times 10^9 Pa} = 6.85168 \times 10^{-9}\ m^4$$

As we use imperial unit system in the finite element modeling, all units expressed in the international unit system need to be converted to those expressed in the imperial unit system.

$$\boldsymbol{E = 6.66 \times 10^6\ psi}, \qquad \boldsymbol{G = 1.252 \times 10^6 psi}$$

$$\boldsymbol{I = 5.098 \times 10^{-3}\ inch^4}, \qquad \boldsymbol{J = 1.646 \times 10^{-2} inch^4}$$

Since we are not interested in the beam in-plane bending, we can assume the in-plane bending area moment of inertia to be a very large value,

[††] Table 17 in the UMN spar built and test report

$$I_{inplane} = 15.29\ inch^4$$

The optimal cross section dimension of BFF's[1] is considered for the mAEWing1 solid spar area,

$$A = 3\times 0.256 = 0.7678\ inch^2$$

It is important to note that the wing inner section that shares the body flap with the fuselage is stiffened at the two edges, shown in Figure 4. As there are no available values for bending stiffness, cross-sectional area and torsional stiffness for this stiffened member. The out of plane bending area moment of inertia, cross-sectional area and torsional stiffness are, respectively, assumed to be a larger value than that of the beam properties in the outer wing,

$$I = 9.098 \times 10^{-2}\ inch^4, \qquad J = 0.2\ inch^4, \qquad A = 0.9\ inch^2$$

The density of the material for the solid spar was $\rho = 1251.77\ \mathrm{kg/m^3}$ based on BFF's optimal value, which is $\rho = 0.04522\ \mathrm{lb/in^3}$ obtained from reference [1].

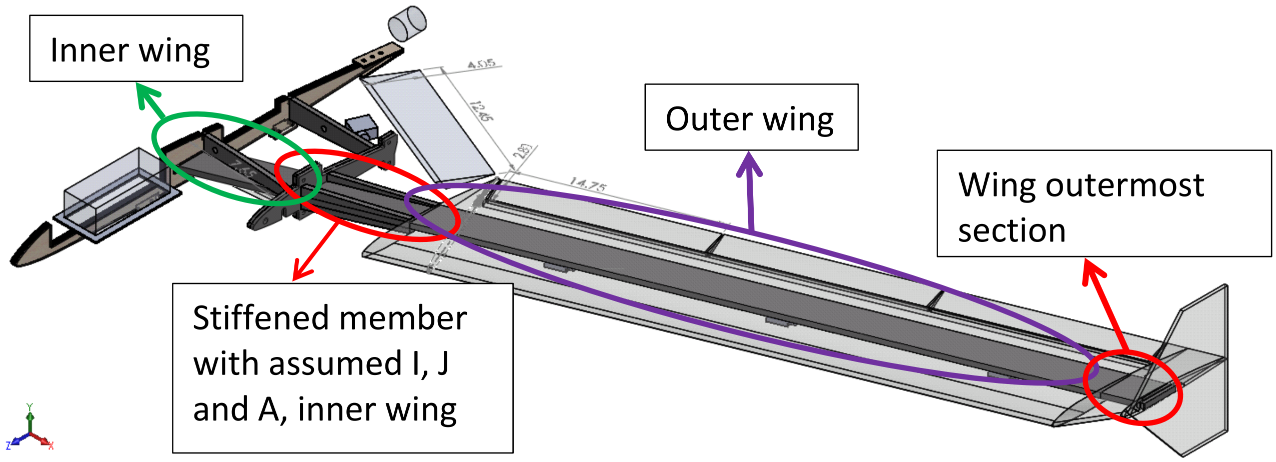

Figure 4 Stiffened spar for the inner wing which shares the body flap with center body

It was found that the foam cover contributes the torsional stiffness to the whole wing of the BFF model. So, the foam torsional stiffness should be taken into account in the wing modeling. But the bending stiffness of the foam can be neglected. The torsional stiffness J for the beam properties in the outer wing section is assumed to increase to $J = 2.146 \times 10^{-2}\ inch^4$.

The foam cover is made of XPS, whose density value is $\rho = 2.584 \frac{lb}{ft^3} = 1.4953\ lb/in^3$[2]. The volume of the foam cover can be figured out in SolidWorks, and then the weight of the foam cover can be obtained.

The foam cover weight is assumed to distribute uniformly to the solid spar. These weight are considered as non-structural mass (NSM) in the beam properties for the solid spar. The unit for the non-structural mass value is pounds per unit length. These values are obtained by the total weight value of each section in the inner wing, outer wing and wing outermost section, dividing the total beam elements length in each section.

From the CAD model, the CG location for the foam at the outer wing section doesn't locate at the elastic axis. So, it is necessary to consider the mass moment of inertia due to the offset between the foam cover CG with the EA. So, there are some scalar mass elements used to taken into account of the foam mass moment of inertia w.r.t the elastic axis in the beam modeling for the outer wing section.

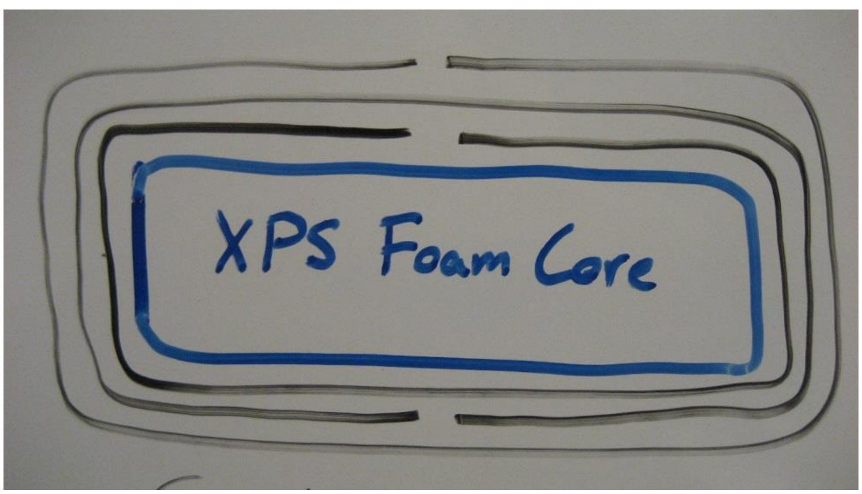

Figure 5 XPS used for the foam cover

As there are 4 sections along each wing, center body, inner wing, outer wing and wing outermost section. The foam cover for the semi-wing was divided into 4 parts and their values are shown in Table 4. These 4 nonstructural mass values will be added to the beam properties for the 4 sections.

Table 4 Non-structural mass values for beam elements (lbs/in)

section	center body	inner wing	outer wing	wing outer most section
value	0.03764	0.015728	0.00939	0.0067

Several considerations in the finite element modeling of mAEWing1 are considered:

- The elements for the outer section of the wing, with 3 flaps, are obtained by discretizing this part into several uniform beam elements. (12 in mAEWing1 FEM v1)
- The inner section of the wing, which shares the body flap with the fuselage, has two uniform beam elements.
- The fuselage, i.e. center body, has two uniform beam elements.
- For the wing outer most section, from the CAD model, this small part is not uniform along the span, there is one beam element for that part. Equivalent cross sectional area, equivalent EI and GJ were considered for this element.

- For the centerline that has a battery, the flight computer and a motor, except the two nodes at the nose and tail, there are 3 yellow nodes used to represent the CG location of each component and these components are modeled as point masses, and one more purple node that connects the bar through fuselage.

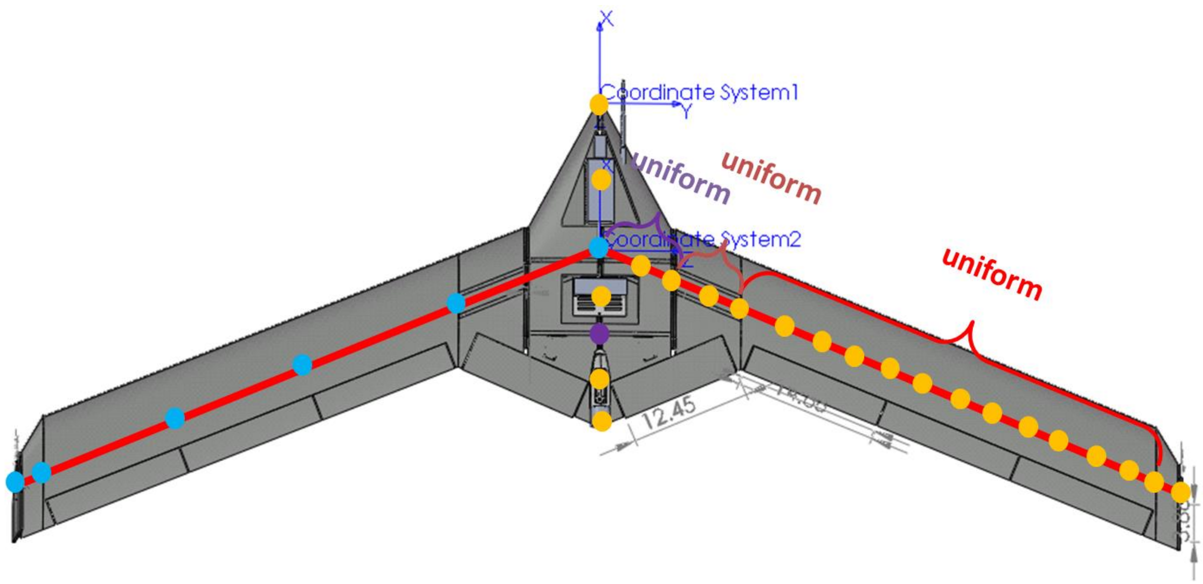

Figure 6 Finite element nodes in the right wing is considered in the mAEWing1 FEM

2) Modeling of Fuselage

The fuselage was modeled as a rigid bar along the centerline. From the CAD model, there are 4 attachments along the centerline and there are some instruments including flight computer, battery and motor located along the centerline.

The rod elements used to model the centerline are assumed to have an equivalent rectangular cross section. We need to know the geometric dimension of the rectangular cross section. These four attachments have 0.5” width, the total volume and length can be obtained in CAD model, the equivalent cross sectional area found from the CAD model is approximate 0.844 in^2, then the equivalent height for the rectangular cross section is calculated to be approximately 1.688". The material for the rod element is also considered as same as that for the wing solid spar.

The instruments along the centerline are modeled as point masses with their locations at the CG of each component. From the CAD model, we can get an equivalent CG location of each component. The assumed weights for these point masses are shown in Table 5.

Table 5 Assumed weight for flight computer, batteries and engine motor[‡‡]

Component	**Flight computer**	**Batteries**	**Engine motor**
Weight	0.513lb	0.50 lb	0.441 lb

[‡‡] The weight for flight computer and motor are from AIAA-2015-0903 paper, weight for batteries are a guess value to match the total vehicle with BFF’s, they are subject to change based on GVT data

3) Modeling of Control Surfaces

There are 2 body flaps and 6 control surfaces attached to the mAEWing1. Each control surface or body flap is modeled as a point mass with mass moment of inertia about the hinge line.

There are 2 local coordinate systems developed to describe the body flap deflection and control surface deflection in each wing, both have y-axis along the hinge line.

There are two other massless points located at the two edges of each control surface or body flap with rigid connections to the point mass element. These massless points are mainly used for aeroelastic spline.

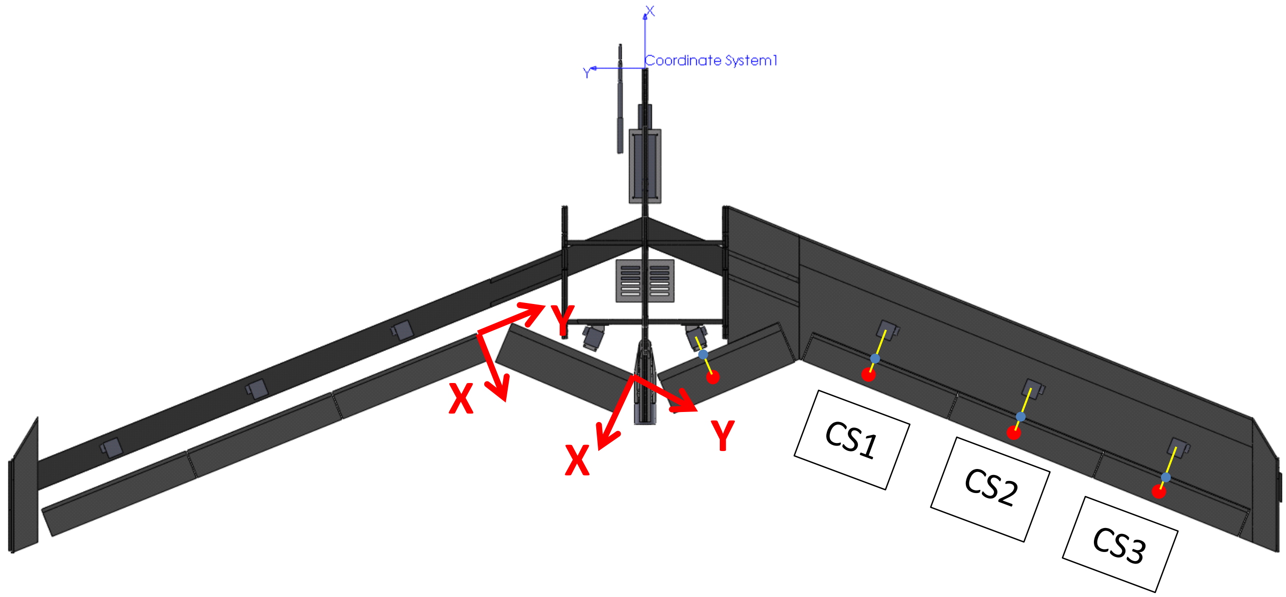

Figure 7 Local coordinate system for control surface with y-axis long the hinge line

It is important to note that in the control surface/body flap modeling, as sensor controls the flap through a rod that is perpendicular to the hinge line, as shown by the yellow line in the right wing represented in the Figure 5. The point mass location, red points in the Figure 5, doesn't represent the CG location of each control surface/body flap. So, the additional mass moments of inertia due to the offside between the point mass location and the flap CG location should be considered in the flaps point mass modeling.

To add a mechanism for the control surface, there are rotational springs exist in the hinge line that connect the flaps with the main wing, seen the blue points representing the location of the spring in the right wing in the Figure 7. So, the hinge bolts that connect the flaps to the main wing are modeled as spring elements as shown in Figure 8.

In the Figure 8, there are two points fore and aft the hinge line located in the main wing and flaps, respectively. They are connected through a very stiff spring. These two points near the hinge line are very close to each other. They are connected to the main wing and flaps points through rigid bar connections, respectively.

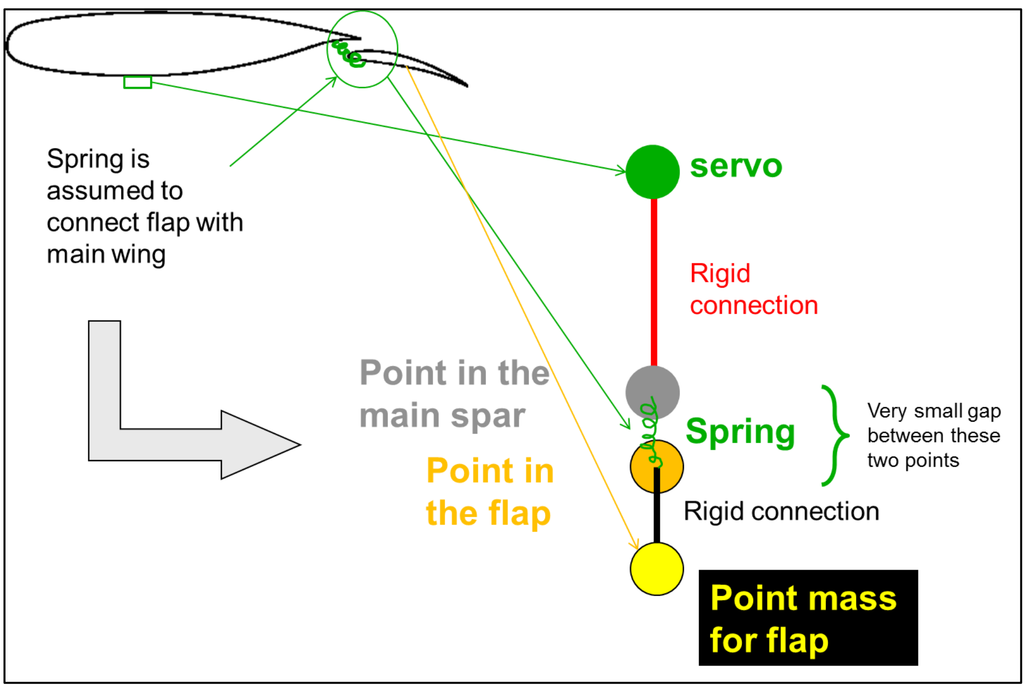

Figure 8 Modeling of sensors and effectors in mAEWing1 FEM

As the values for the spring stiffnesses are not available now, the value for the rotational spring stiffness was assumed to be a large value in the current finite element model. These values are subject to change to reflect the real spring stiffness.

$$k_{bf} = 10^6 \ lbs - in/rad$$

$$k_{cs,1} = 10^6 \ lbs - in/rad$$

$$k_{cs,2} = 10^6 \ lbs - in/rad$$

$$k_{cs,3} = 10^6 \ lbs - in/rad$$

All actuators are anticipated to be the Futaba S9254 with a bandwidth of 10.5 Hz, the weight for this type of actuator is assumed to be 0.126 lbs [3].

4) Modeling of Winglet

Winglets are also modeled as the point mass elements located at the wingtip beam element node. As there is an offset between the winglet CG and the beam node as seen in Figure 9, the mass moment of inertia due to this offset is included in the point mass element.

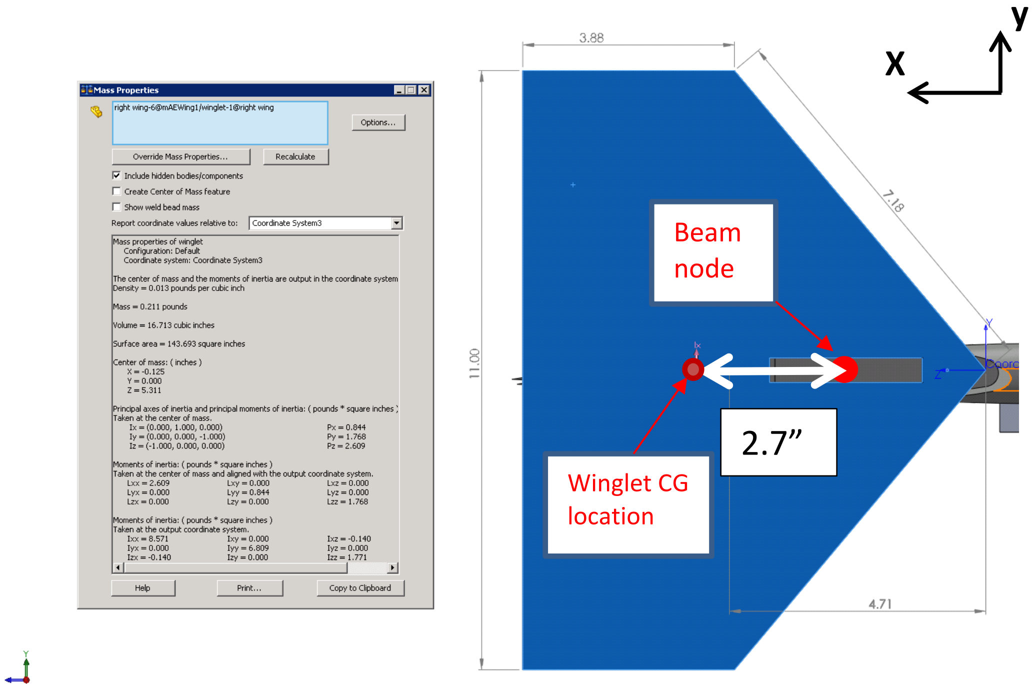

Figure 9 CG location and mass properties of winglet

The weight for the winglet is assumed to be 50g, around 0.11023lbs [1], and has an offset about 2.7” with the wing tip beam element node along the x-axis.

5) Miscellaneous

a) Wing attachments

For each wing, there are two wing attachments as shown in Figure 10. One is used to connect the outer wing with the inner wing. Also there are two rods connecting the wing attachment in each side of the fuselage centerline to stiff the center body. This wing attachment in each wing is modeled as rod elements. Like the modeling of the center attachments, the equivalent rectangular cross section with width 0.5” and height 1.48” is considered for these two rod elements, the values for the width and the height of this wing attachment are obtained similarly to those for the center attachments as shown in section 2).

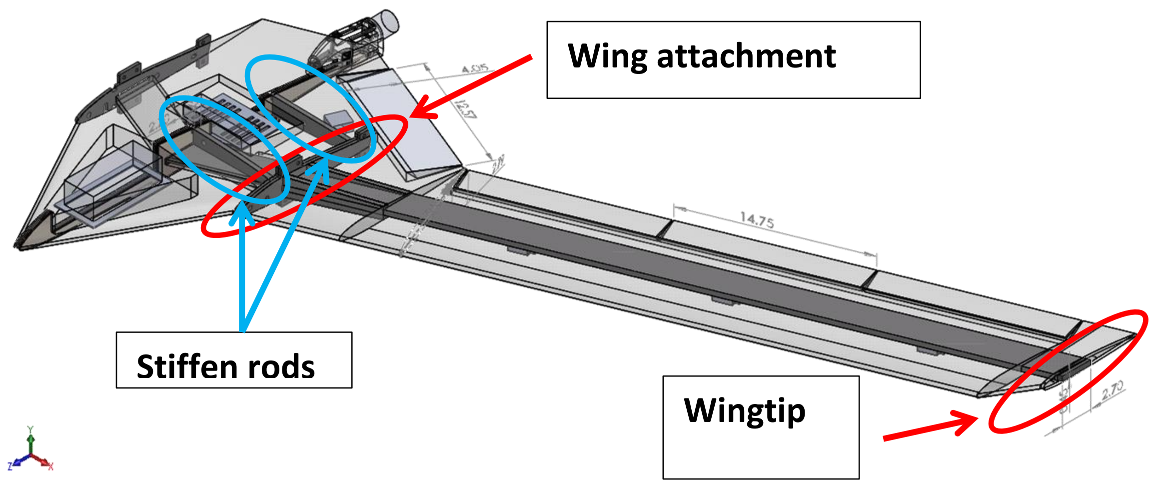

Figure 10 Two wing attachments in each wing

The other one that connects the wing and the winglet is modeled as a point mass with its location is at the wingtip beam element node with an offset value around 1.3” between the CG of this wing attachment and the wingtip beam element node.

There are some massless points considered to model the shape of the winglet in each wing, which are located in the corners of the winglet. They are connected to the winglet point mass element through rigid bar connections. These massless points are mainly used in the aeroelastic spline.

b) Servos

All servos are modeled as point masses with their locations at their center. It was found their centers are very close to the elastic axis. So, the locations of all servos are considered in the elastic axis. The value for the weight of each servo is assumed to be 10g [3].

c) Stiffened member

There are three small spars used to stiff the fuselage, the front two top and bottom spars are equivalent as one spar in the FEM. Both the front spars and the rear spar in the fuselage are modeled as beam elements with a very large out of plane bending stiffness value. Their beam properties are shown in the Table 6.

Table 6 Beam properties for front and rear spars in the fuselage

Properties	$A, inch^2$	$I_{out}, inch^4$	$I_{in}, inch^4$	$J, inch^4$
front spar	0.686	39.322	5.179e-2	3.165
rear spar	0.482	24.322	5.179e-2	1.105

d) pitot tube

The pitot tube is modeled as a point mass element with weight value 0.002lb. Its location is in the center of the pitot tube.

e) Accelerometer

mAEWing1 CAD model doesn't have the accelerometers now, so estimations of the accelerometers locations are referred to the BFF's [3].

6 Accelerometers are mounted in the BFF vehicle. Each aligned to the vertical axis. The center body aft accelerometer is the only one visible and is identified as an Endevco7290A-50. The 7290A mass is listed as 12 grams plus 9 grams/meter for the cable according to the spec sheet. The accelerometer positions were estimated from using the utility "*grabit.m*" in MATLAB as shown in Figure 11. Left-Right symmetry was enforced artificially. The origin for measurements is the aircraft nose; X is forward, Y is out the right wing.

Table 7 Accelerometer Type and Position for BFF model

Accelerometer	Type	Position X (+forward) (inches)§§	Position Y (+right) (inches)
Centerbody For	Unknown	-2.3 (-13.25)	0.0
Centerbody Aft	Endevco7290A-50	-24.9 (9.35)	0.0
Left Wing For	Unknown	-33.3(17.75)	-54.3

§§ The reference system used in this table with the origin defined in the nose of the BFF. The values in the parenthesis are for the x coordinates in the mAEWing1 FEM with the origin at the elastic axis. y axis coordinates are same in BFF FEM and mAEWing1 FEM.

Left Wing Aft	Unknown	-39.5 (23.95)	-54.3
Right Wing For	Unknown	-33.3 (17.75)	54.3
Right Wing Aft	Unknown	-39.5 (23.95)	54.3

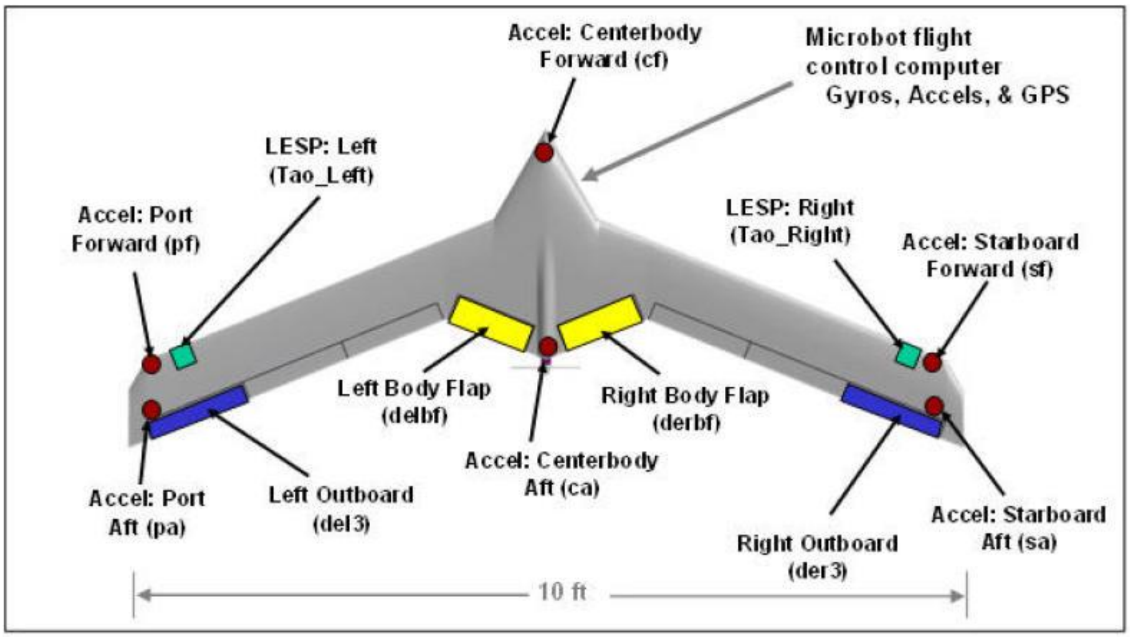

Figure 11 The BFF Vehicle

All accelerometers are modeled as point mass elements with the weight value to be 12g. They are connected to the main wing through rigid bar connection.

D. NASTRAN mAEWing1 Beam-rod FEM v1.1

Mimic the mAEWing1 CAD model and base on the data summarized in previous sections, the NASTRAN beam-rod FEM of the mAEWing1 is developed. As the solid spar has rectangular cross section, we assume the E.A. is through its center, so that we developed the beam rod model for mAEWing1 as shown in Figure 12.

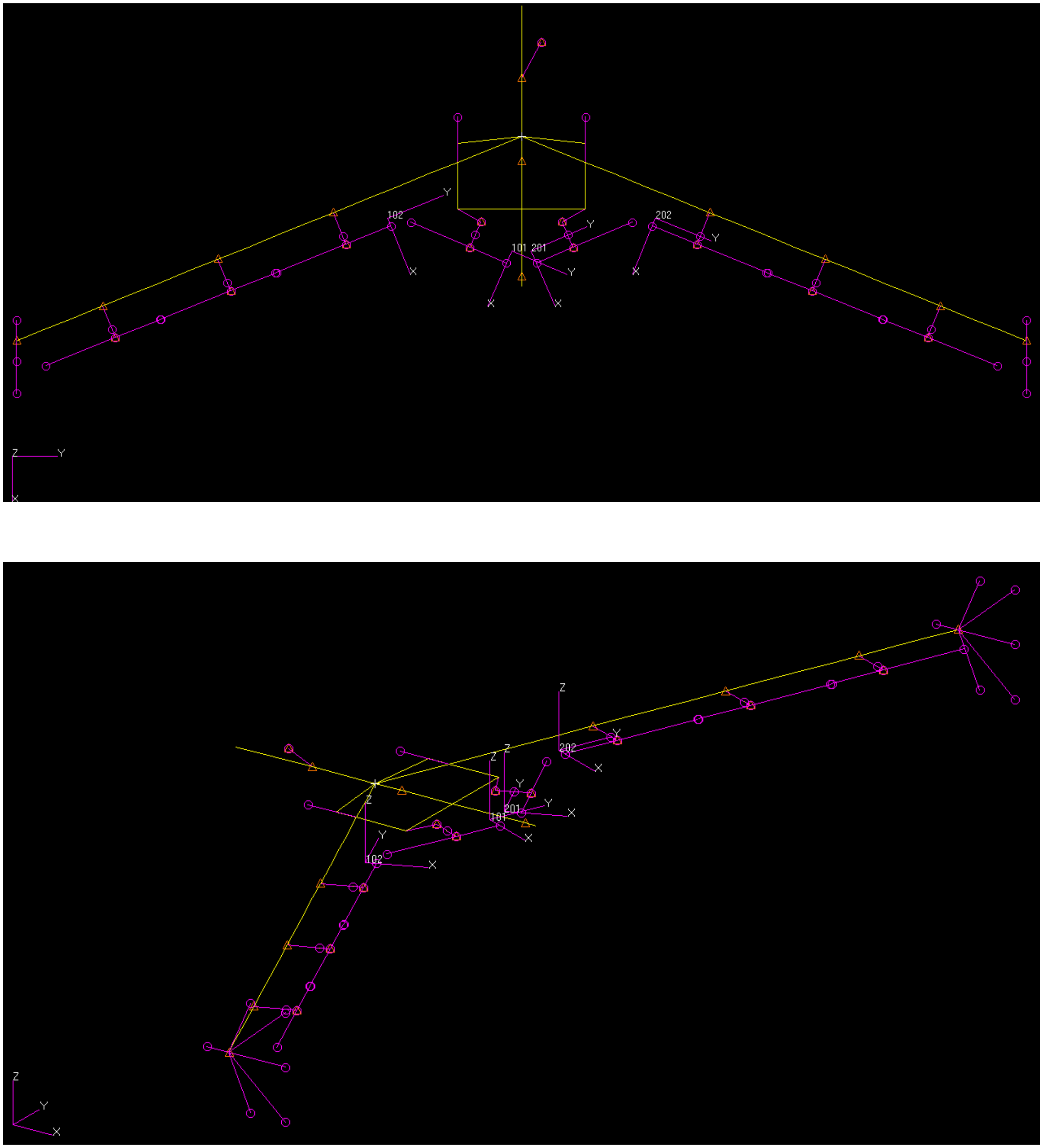

Figure 12 Finite element beam-rod model of mAEWing1 v1.1 (subject to update)

Finite element model summary in mAEWing1 FEM v1.1

Table 8 Summary of FEM v1.1 of mAEWing1 (***will be updated***)

Element	Number
BAR elements	11
BEAM elements	38
Spring elements	8
Point mass elements	38
Nodes number (mass + massless points)	103
Rigid connection elements	47

E. NASTRAN normal mode results (*will be updated*)

In the NASTRAN normal mode analysis, there are two steps considered. The CG location is calculated first, and then we specify a factious support at the CG location by using SUPORT card, all the 6 degrees of freedom are supported.

The preliminary results related to the mass properties and mode results are presented as shown in Table 9 and Table 10.

The first 12 mode shapes are depicted as shown in Figure 16 to Figure 19.

Table 9 MASS properties for mAEWing1 FEM v1.1

Property	**mAEWing1**	**BFF**

Total weight, lb	12.022	11.99
C.G. location (From nose), inches	25.04	23.29
Pitching moment of inertia, Iyy, lb-in^2	1148.58	1245.83
Rolling moment of inertia, Ixx, lb-in^2	9502.63	8529.45

Table 10 Mode frequencies comparison FEM v1.1

mAEWing1 Modes	**mAEWing1 (Hz)**	**BFF (Hz)**
6 Rigid modes	**0.00**	0.00
1^{st} Sym bending mode	**5.450**	5.67
1^{st} A/S bending mode	**8.602**	8.37
1^{st} Sym torsion mode	**17.96**	18.44
1^{st} A/S torsion mode*	**16.85**	19.82
2^{nd} Sym bending mode	**21.25**	23.17
2^{nd} A/S bending mode	**29.32**	28.60
A/S - Anti-symmetric; ST- Symmetric Torsion; AST - Anti-symmetric Torsion **Lower frequency for 1^{st} AS torsion mode for mAEWing1 FEM v1*		

Mode	Frequency, Hz	Mode shape	descriptions
1	0.000	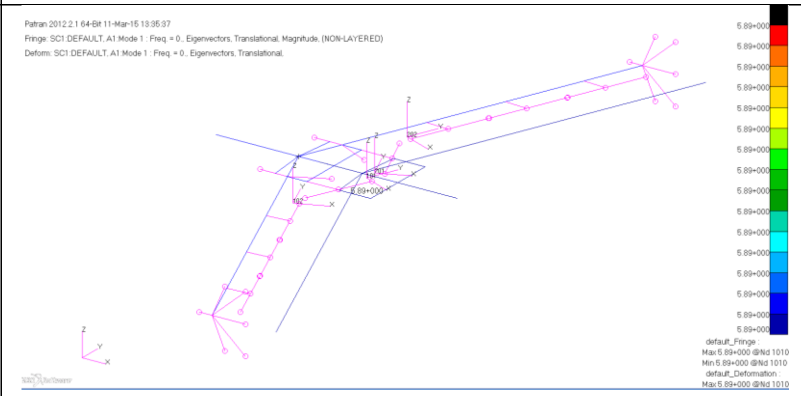	Rigid translational mode along x-axis
2	0.000	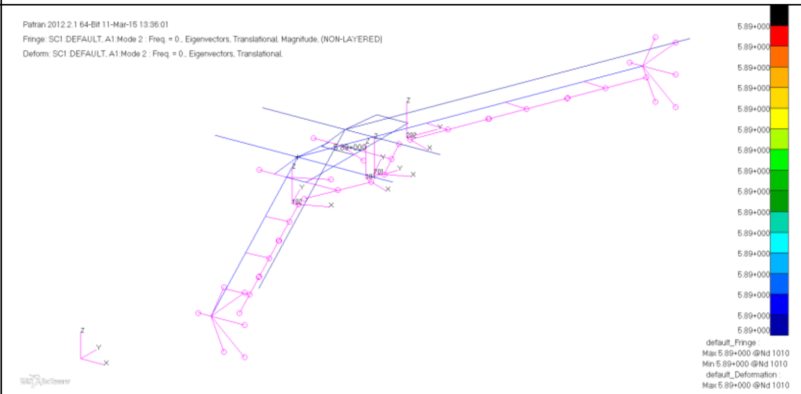	Rigid translational mode along y-axis
3	0.000	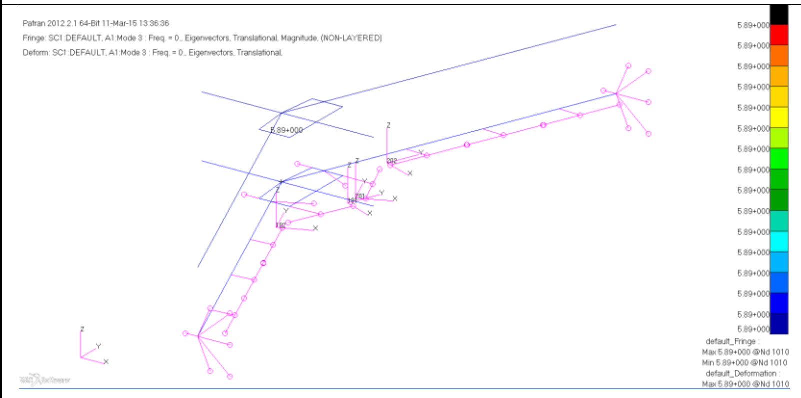	Rigid translational mode along z-axis

4	0.000	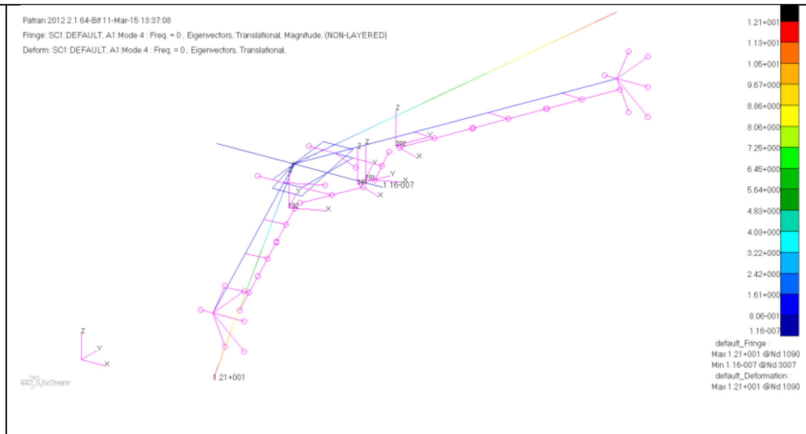	Rigid roll mode
5	0.000	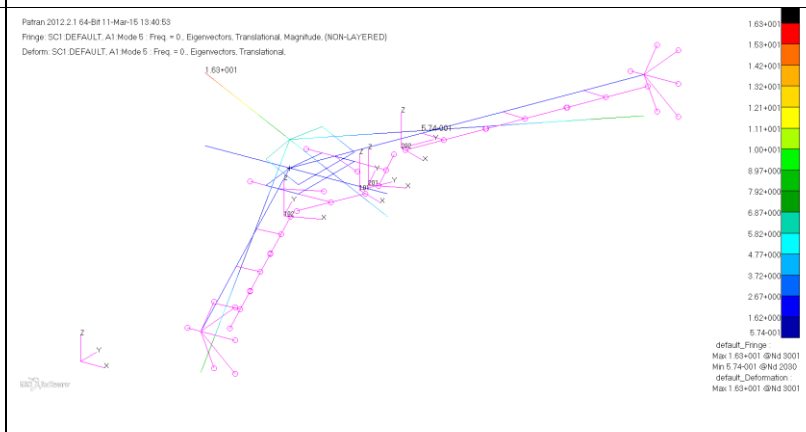	Rigid pitch mode
6	0.000	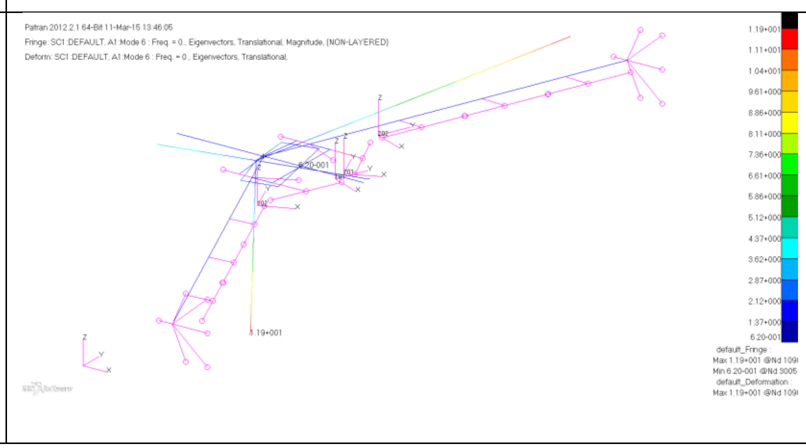	Rigid yaw mode

Figure 13 The 6 rigid modes mode shape of mAEWing1 FEM v1.1

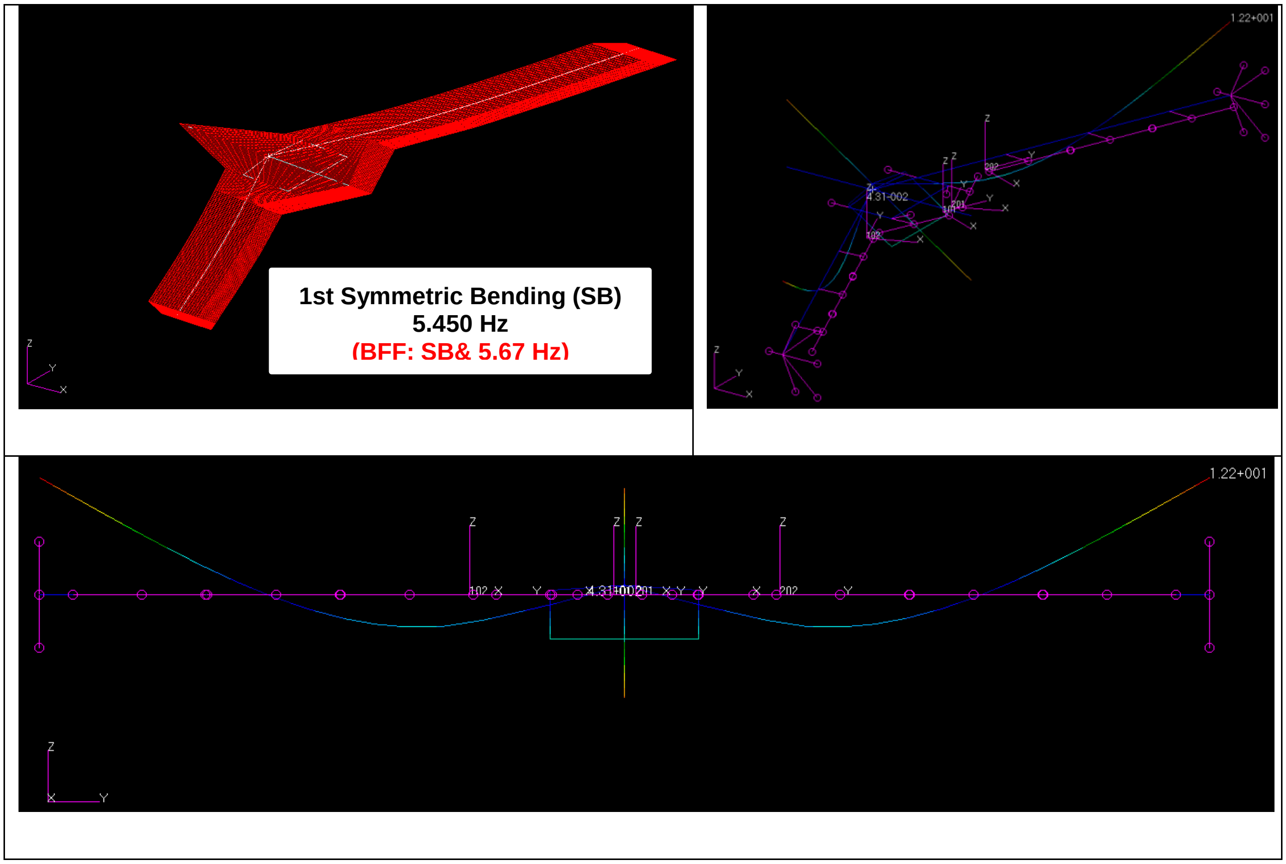

Figure 14 The first symmetric bending mode, mode 7

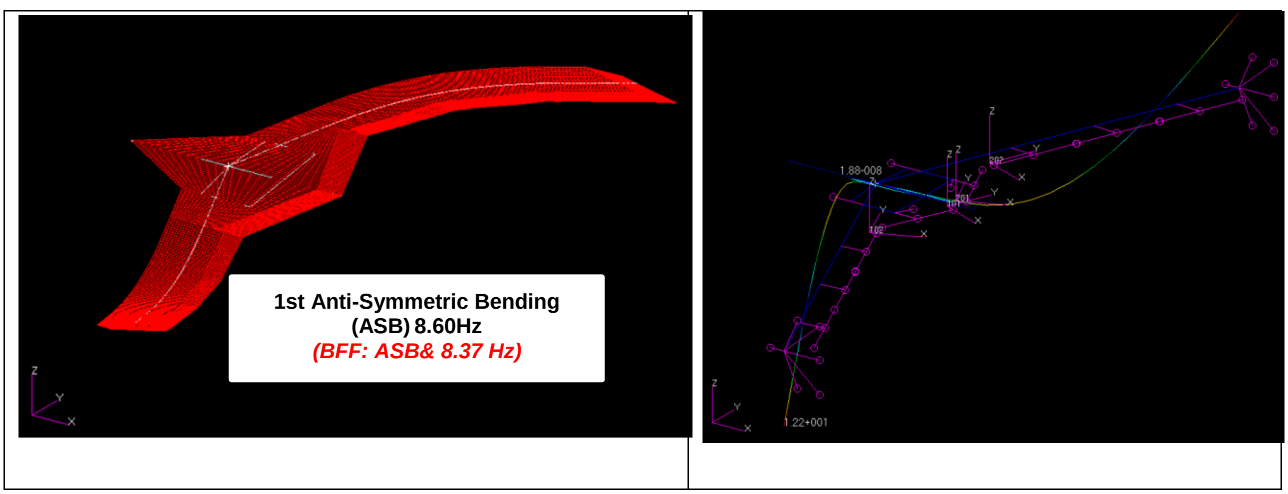

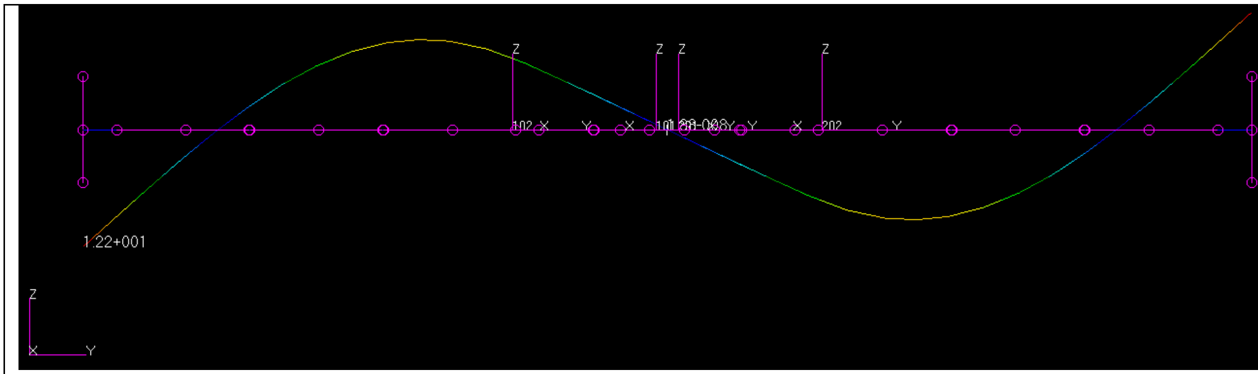

Figure 15 The first antisymmetric bending mode, mode 8

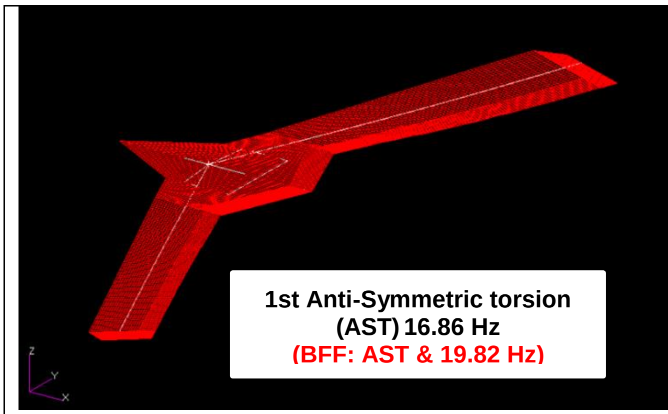

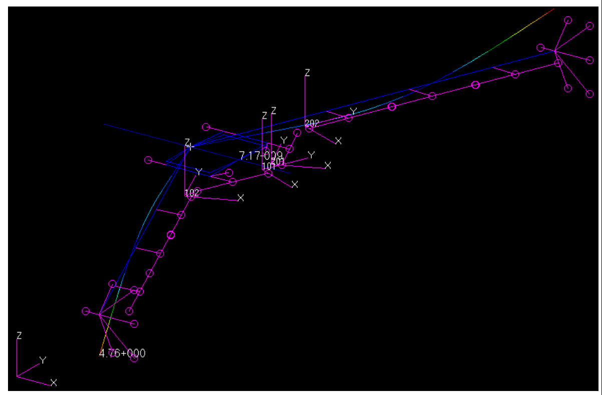

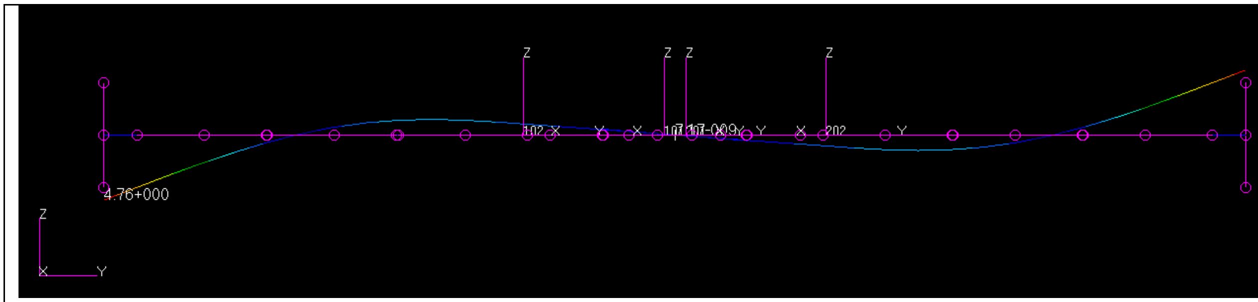

Figure 16 The first antisymmetric torsion mode, mode 9

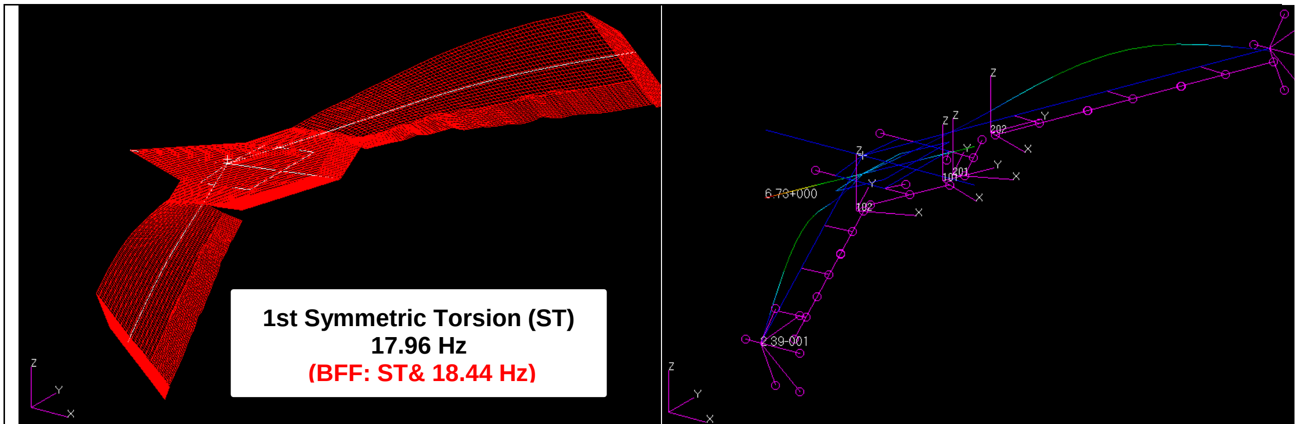

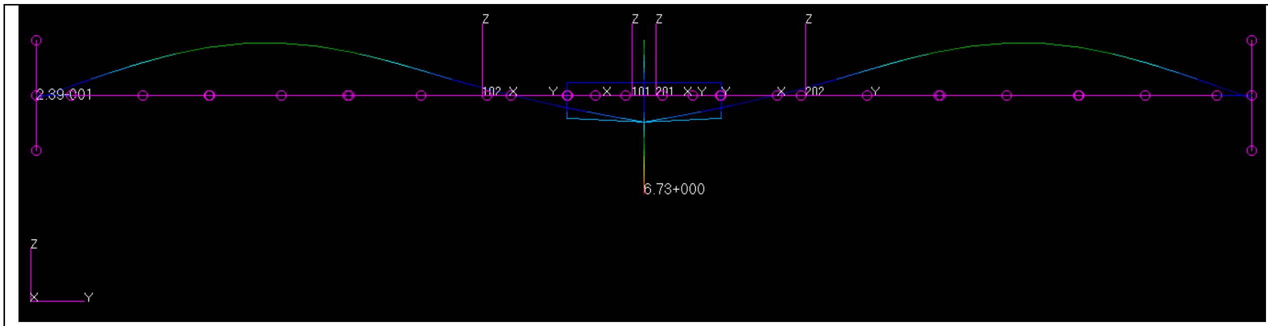

Figure 17 The first symmetric torsion mode, mode 10

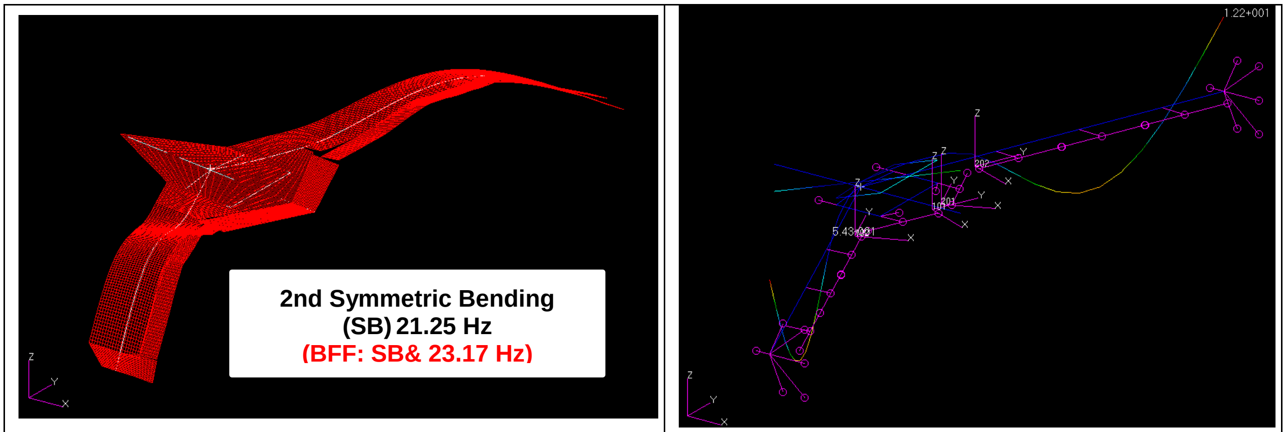

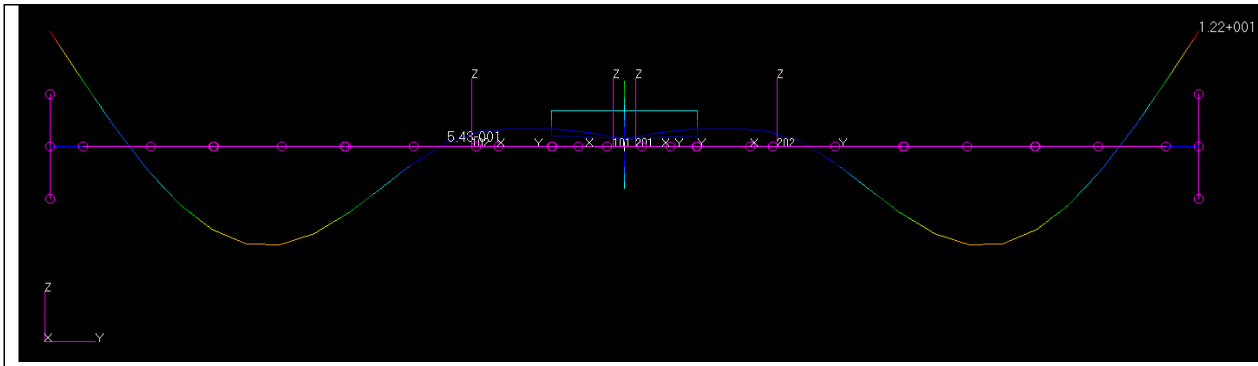

Figure 18 The second symmetric bending mode, mode 11

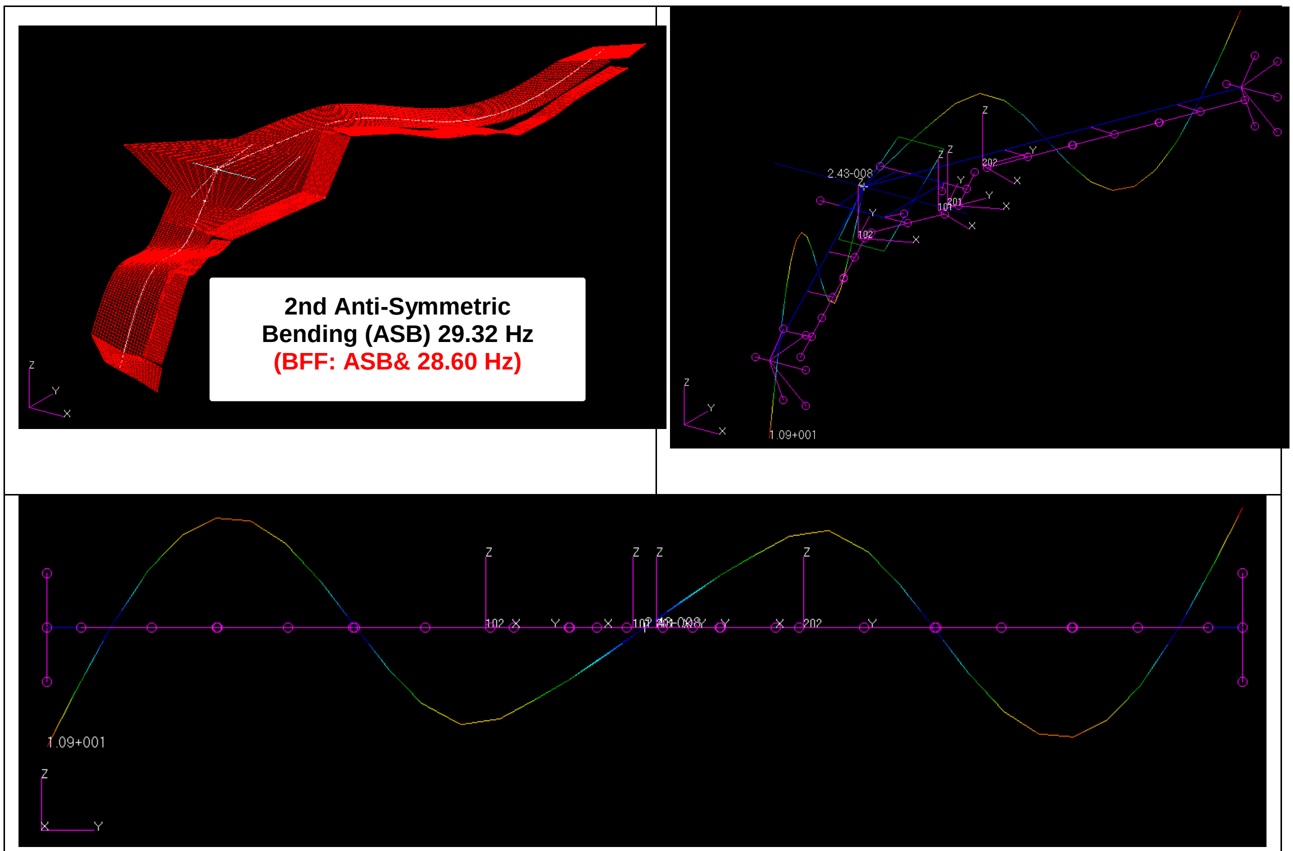

Figure 19 The second antisymmetric bending mode, mode 12

Reference

[1]. Gupta, A., Moreno, C.P., Pfifer, H., and Balas, G. J., *Updating a Finite Element Based Structural Model of a small flexible aircraft*, SciTech2015

[2]. Regan, C., mAEWing1 - Spar Design, Build and Test, 2015

[3]. Aircraft Data_v0.1_BFF - Build Description downloaded from www.paaw.net, 2015

[4]. Edward L. Burnett, Christopher Atkinson, et al., *NDOF Simulation Model for Flight Control Development with Flight Test Correlation*, AIAA Modeling and Simulation Technologies Conferences, August, 2010

Appendix

1. NASTRAN finite element model files, including input bdf file, output f06 file and PATRAN database file.(will be uploaded to Dropbox)